Lithuanian Journal of Physics
Vol. **66**, No. 3, pp. 137–145 (2026)

ISSN 1648-8504 eISSN 2424-3647
DOI: https://doi.org/10.3952/physics.2026.66.3.1

PREPARATION AND CHARACTERIZATION OF CARBON–SILVER NANOSTRUCTURES

U.K. Makhmanov [a, b], X. Jiang [c], J. Yang [c], and T.A. Chuliev [a]

[a] *Institute of Ion-Plasma and Laser Technologies, Uzbekistan Academy of Sciences, 33 Durmon Yuli Street, 100125 Tashkent, Uzbekistan*

[b] *National University of Uzbekistan named after Mirzo Ulugbek, 4 Universitet Street, 100174 Tashkent, Uzbekistan*

[c] *International Chinese-Belorussian Scientific Laboratory on Vacuum-Plasma Technology, Nanjing University of Science and Technology, 200 Xiaolingwei Street, 210094 Nanjing, China*

Email: urolmakh@gmail.com

Received 5 August 2025; revised 7 February 2026; accepted 16 April 2026

The creation of nanocomposite materials based on fullerene and a rare metal with unique hybrid properties is promising for use in chemical sensors, photocatalytic devices and energy storage devices. A nanocomposite thin film containing fullerene C_{60} and silver (Ag) nanoparticles was synthesized by introducing an Ag nanoparticle into the fullerene matrix using thermal evaporation of the solution. The morphological and optical properties of both solutions consisting of fullerene and silver and the C_{60}–Ag nanocomposite at different concentrations of the components were studied using optical absorption, refractometry, dynamic light scattering, Raman spectroscopy and electron microscopy. The surface plasmon resonance (SPR) band of the C_{60}–Ag nanocomposite under different conditions was determined. A significant redshift (~12 nm) of the SPR band was observed with annealing a thin film at 60°C.

Keywords: C_{60}, silver nanoparticles, multicomponent solution, nanocluster, one dimensional material, nanocomposite, surface plasmon resonance

PACS: 61.46.Bc, 81.05.Tp

1. Introduction

Today, semiconducting carbon nanostructures of various sizes are widely used to create nanoelements for biomedicine, microelectronics, optoelectronics, nanotechnology, solar energy, and nanoelectromechanical devices [1–2]. In this regard, fullerenes are becoming the main components of nanotechnology for the creation of functional nanostructures [3–4]. Particularly stable fullerenes (C_{60}, C_{70}) are distinguished by their excellent electron acceptor properties, high photosensitivity and high electron mobility [5–6]. Currently, the creation of nanocomposite materials based on fullerene nanostructures and the study of their properties are also continuing at a rapid pace.

As a way to expand the practical application of fullerene-based nanomaterials, it is possible to propose, for example, finding optimal options for synthesizing metal–fullerene nanocomposites. When fullerene nanostructures are coated with various rare metal nanoparticles, their optical, electrical and antibacterial properties are further improved [7]. As a result, it will be possible to create nanocomposite materials with unique hybrid properties, promising for use in relatively compact light sources, chemical sensors, energy collection and storage devices, and photocatalytic devices [8–9]. Among rare metals, silver (Ag) is a promising metal for photocatalytic and energy conversion due to its stability, high electrical conductivity, low cost and non-toxicity [9]. In addition, silver nanoparticles are of interest due to local plasmon resonance, which leads to a strong absorption of light at a specific wavelength in the visible region [10]. To achieve the multifunctional properties of these nanocomposites, it is necessary to control the concentration of Ag in the composite. In this case, the concentration of Ag should be as small as possible, but at the same time, the atomic concentration of the metal should be kept high enough to form nanoparticles in the fullerene matrix. The main issue is to keep the degradation of fullerene properties to a minimum. The reduced reactivity of stable fullerenes, especially C_{60}, with silver nanoparticles makes nanocomposites based on them particularly interesting for plasmonic integrated devices [11–12]. At the same time, fullerene C_{60} is relatively inert and hydrophobic, while silver is reactive and has antimicrobial properties, so they are one of the most promising types of nanomaterials to date [13–14]. One of the main problems is to control the size and shape of silver nanoparticles that are applied to the fullerene surface. The size and shape of nanoparticles significantly affect their properties, so it is important to ensure their uniform distribution and specified parameters.

In this paper, we study the synthesis of nanostructures consisting of fullerene C_{60} and Ag, as well as their optical, structural and morphological properties. Experimental methods for controlling the optical properties (in particular, surface plasmon resonance) of the synthesized supramolecular structures are discussed.

2. Samples and techniques

In the experiments, solutions of fullerene C_{60} and silver with different concentrations were used. Silver nitrate ($AgNO_3$, ACS reagent, ≥99.0% purity) and fullerene (C_{60}) (99.9% purity) nanoparticles were purchased from *Sigma Aldri*ch (USA). Analytical grade solvents used in the experiments – orthoxylene (C_8H_{10}, hereinafter referred to as xylene), ethanol (C_2H_6O), polyvinyl pyrrolidone ($(C_6H_9NO)_n$) and ethylene glycol ($C_2H_6O_2$) were purchased from *Sigma Aldrich* (USA). The true solution of C_{60} in 20 ml of xylene was prepared by dissolving fullerene to the molecular state using a magnetic stirrer at a frequency of 2.0 Hz for 2 h. In this case, the initial concentration of C_{60} in the solution was ~0.2 mg/ml.

The polyol method was used to synthesize silver nanoparticles. First, a solution of polyvinyl pyrrolidone in ethylene glycol was prepared as a stabilizing agent. For this, ethylene glycol was heated to 72°C, then polyvinyl pyrrolidone was added and stirred for 15 min using a magnetic stirrer. The prepared solution was removed from the oven and cooled to room temperature. Then, silver nitrate ($AgNO_3$) was added to the solution and stirred for 0.5 h at room temperature. The solution was placed in an oven at 135°C and kept for 10 min. Then, the solution was removed from the oven and cooled to room temperature. The synthesized silver nanoparticles were separated from the solution using a centrifuge. Thus, crystalline silver powders with particle diameters of <100 nm were obtained. C_{60}/Ag/xylene/ethanol solutions with different silver concentrations were prepared by adding Ag/ethanol solutions to C_{60}/xylene solutions. The C_{60} concentration was kept constant.

Ultraviolet–visible (UV–vis) absorption spectra were measured using a *Shimadzu* UV–vis 2700 spectrophotometer (*Shimadzu*, Japan).

The measurement of the precise refractive index (*n*) of the C_{60}/xylene, Ag/ethanol and C_{60}/Ag/xylene/ethanol system was performed at the sodium D_1 line wavelength (~589.3 nm) using a high-sensitivity digital refractometer PAL-BX/RI (*ATAGO*, Japan).

A portable densitometer Densito Pro (*Mettler Toledo*, Japan) was used to measure the density of the solution. The device has an accuracy of ±0.001 g/cm^3 and a resolution of ±0.0001 g/cm^3.

The distribution characteristics of the dispersed phase of fullerene C_{60} and Ag, including the average hydrodynamic size and particle concentration in solutions, were analyzed using dynamic light scattering (DLS) with a Zetasizer Nano ZEN3600 system (*Malvern Instruments Ltd.*, UK).

The structure of studied samples was characterized by a field emission scanning electron microscope (SEM) *Hitachi* S-4800 (Japan).

The Raman spectra of fullerene solutions were recorded using an InVia Raman spectrometer (*Renishaw*, UK). A Cobolt CW 532 nm DPSS laser served as the excitation source, operating at a wavelength of 532 nm.

3. Results and discussion

The refractive index of fullerene and silver solutions varies with both the concentration of the solutes and the solvent used. When light (~589.3 nm) passes through the solution, interactions occur between the photons and the shared electric and magnetic fields created by C_{60}–Ag-solvent molecules. The strength of the interactions depends on the strength of the electric and magnetic fields of solution components. The refractive index and density of the C_{60}/Ag/xylene/ethanol solution at different silver concentrations are given in Table 1. In this case, the fixed concentration of C_{60} is 0.2 mg/ml. It should be noted that the measured refractive index values of C_{60}/xylene and Ag/ethanol solutions at a solute concentration of 0.2 mg/ml are 1.5042 and 1.3639, respectively. It is evident that (see Table 1) with increasing Ag concentration in the solution, the refractive index value in the C_{60}/Ag/xylene/ethanol solution decreases unevenly. This uneven change is particularly noticeable at Ag concentrations of 0.08 and 0.12 mg/ml. In our opinion, this is due to the strengthening of intermolecular interactions of components in the solution, and also, probably, to an increase in the size of fullerene and Ag nanoclusters and a decrease in their number in the solution.

Table 1. Change in the refractive index and density in the C_{60}/Ag/xylene/ethanol solution depending on the concentration of silver nanoparticles. The concentration of C_{60} in the solution is ~0.2 mg/ml.

Silver concentration, mg/ml	Refractive index, n	Density, kg/m^3
0.04	1.5022	876.0
0.08	1.4775	872.6
0.12	1.4819	872.2
0.16	1.4937	872.1
0.20	1.4914	870.6
0.24	1.4888	868.9
0.28	1.4841	867.7

During the experiments, the measured average density values of C_{60}/xylene and Ag/ethanol solutions (dissolved substance concentration 0.2 mg/ml) were 878.8 and 804.1 kg/m^3, respectively. Table 1 shows that the density of the solution decreases with increasing a silver volume fraction in the solution. However, even in this case, it can be seen that at a silver concentration of 0.08 mg/ml, the density of C_{60}/Ag/xylene/ethanol change decreases more than linearly. This also creates a situation similar to the change in the refractive index values and indicates that more intermolecular interactions have occurred.

The absorption spectrum of the synthesized silver nanoparticles (AgNPs) in ethanol is shown in Fig. 1. The spectrum exhibits a well-defined and in-

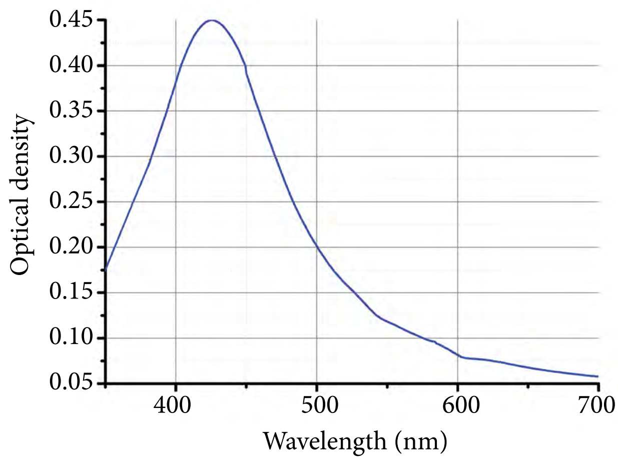

Fig. 1. Absorption spectra of silver nanoparticles in ethanol at a concentration of ~0.12 mg/ml.

tense localized surface plasmon resonance (LSPR) band centred at ~425 nm, which is characteristic of colloidal silver nanoparticles in a size range of roughly 10÷40 nm [15]. This resonance arises from the collective oscillation of conduction electrons in AgNPs under optical excitation, a phenomenon extensively reported for spherical AgNPs in dielectric media such as alcohols and water–alcohol mixtures [16–17]. The narrowness and symmetry of the SPR peak suggest a relatively monodisperse size distribution of the synthesized nanoparticles. The full width at half maximum (FWHM) determined from the spectrum indicates a limited inhomogeneous broadening, implying a minimal variation in particle diameter. The literature shows that small AgNPs (<20 nm) generally exhibit sharper LSPR bands, whereas broader or red-shifted features appear when polydispersity, aggregation, or anisotropic geometries are present [18–20]. The profile observed in Fig. 1 is consistent with a predominantly spherical and weakly aggregated nanoparticle population.

Figure 2 shows the absorption spectra of C_{60}/xylene and C_{60}/Ag/xylene/ethanol solutions at different concentrations of Ag in the solution. The absorption spectrum of C_{60}/xylene solution shows three bands in the visible range at ~406.4, ~531.5 and ~597.4 nm, which correspond to the well-known electronic transitions of molecular C_{60} in weakly polar aromatic solvents [21]. These bands arise from allowed transitions between the $H_u \rightarrow T_{1u}$ and $A_g \rightarrow T_{1g}$ states in the C_{60} molecular manifold and are typically observed in the 400–620 nm region under conditions

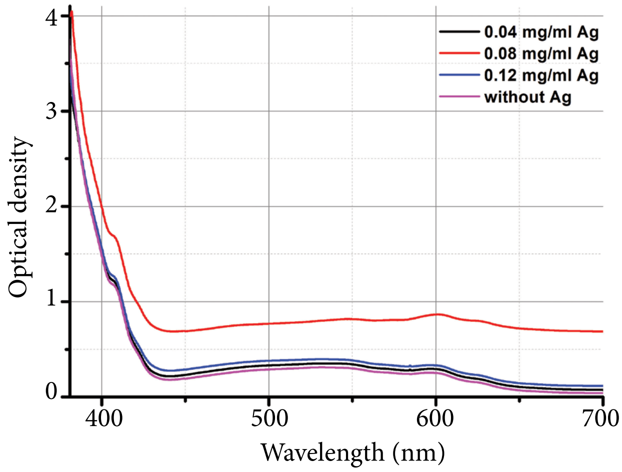

Fig. 2. Absorption spectra of C_{60}/xylene and C_{60}/Ag/xylene/ethanol solutions with different concentrations of silver nanoparticles. The concentration of C_{60} in the solution is 0.2 mg/ml.

where fullerene remains monomeric and well dispersed. It can be seen that the optical absorption is enhanced compared to the C_{60}/xylene solution at 0.04, 0.08 and 0.12 mg/ml of silver concentration in the solution (see Fig. 2). The latter correlates with the plasmonic contribution of AgNPs, the LSPR of which manifests as a broad enhancement superimposed on the C_{60} bands. In addition, small red shifts in the absorption maxima were observed with the addition of Ag to the C_{60}/xylene solution.

AgNPs can locally enhance or redistribute the electromagnetic field, leading to subtle modifications of semiconductor C_{60} absorption structures due to plasmon–exciton interactions and partial quenching processes [22]. A notable feature in Fig. 2 is that the solution containing 0.08 mg/ml of Ag exhibits a higher absorbance across the entire spectral range compared to the solution containing 0.12 mg/ml of Ag, despite the latter having a higher nominal silver content. To understand this behaviour, Fig. 3 provides DLS size distribution curves for both hybrid solutions: 0.12 mg/ml (curve *1*) and 0.08 mg/ml (curve *2*). It is evident from the graph that at both silver concentrations the sizes of clusters synthesized in the solution are polydisperse. At a concentration of 0.12 mg/ml Ag, the dispersion shows relatively small hydrodynamic sizes and narrow line widths, with dominant fullerene–silver cluster sizes at 14, 23, 60, 89, 126 and 168 nm (Fig. 3). These well-defined modes indicate that the nanoparticles and fullerene clusters remain comparatively finely dispersed, with a weaker aggregation. Under such conditions, the interparticle distances are sufficiently small for plasmon coupling and mode damping to occur, and this suppresses the dipole plasmon resonance and reduces the overall optical absorption. The formation of many small clusters enhances light scattering, which is registered by the spectrophotometer as a decrease in absorbance [23].

In contrast, at 0.08 mg/ml Ag, the DLS data reveal that smaller particles aggregate into larger

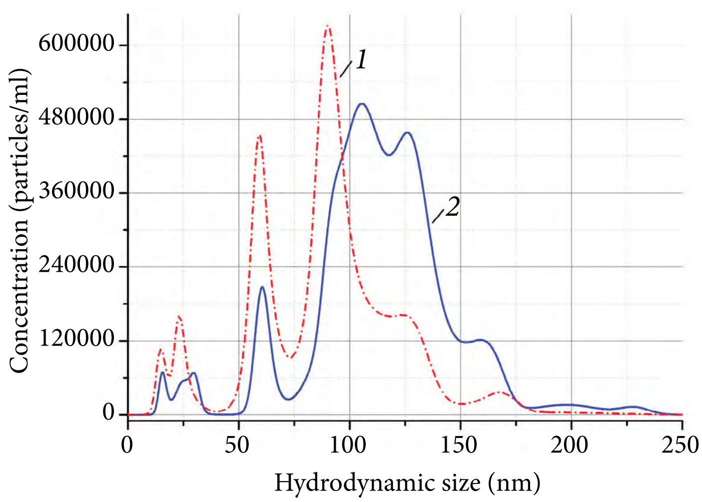

Fig. 3. The size distribution spectrum of the C_{60}/Ag/xylene/ethanol solution with different concentrations of silver nanoparticles: *1*, 0.12 mg/ml; *2*, 0.08 mg/ml. The concentration of C_{60} in the solution was 0.2 mg/ml.

composite structures, producing dominant cluster sizes at 25, 29, 61, 105, 126, 159, 197 and 228 nm (Fig. 3, curve *2*). Although the hydrodynamic sizes are significantly larger, these clusters are looser, more fractal-like, and contain fewer closely packed AgNPs per cluster. Such larger but less compact fullerene–silver clusters preserve the dipolar plasmon resonance of individual Ag nanoparticles more effectively than the smaller, more compact clusters formed at 0.12 mg/ml [24–25]. As a result, the plasmonic absorption is stronger, the local electromagnetic field enhancement is greater, and the fullerene transitions remain more pronounced. This produces a higher optical density compared to that of the 0.12 mg/ml sample (see Fig. 2).

Next, thin films based on fullerene and silver were obtained by thermal evaporation at 45°C, and their characteristics were studied.

Figure 4 presents the SEM image of a thin film of C_{60}–Ag. The SEM image reveals a heterogeneous nanostructure consisting of elongated fullerene nanowhiskers (C_{60}NWs) and high-contrast Ag-containing nanoclusters distributed across the film surface. Rod-like crystalline structures with a length of 4 μm and a diameter of 200 nm are characteristic of C_{60}NWs formed by anisotropic crystallization under low-temperature, supersaturated conditions. The bright quasi-spherical nanosphere domains (with a diameter of up to 400 nm) represent silver nanoparticles, and their spatial co-localization with the C_{60}NWs network (see Fig. 4) suggests that Ag nanoparticles act as heterogeneous nucleation sites and promote the local ordering and growth of one-dimensional fullerene structures.

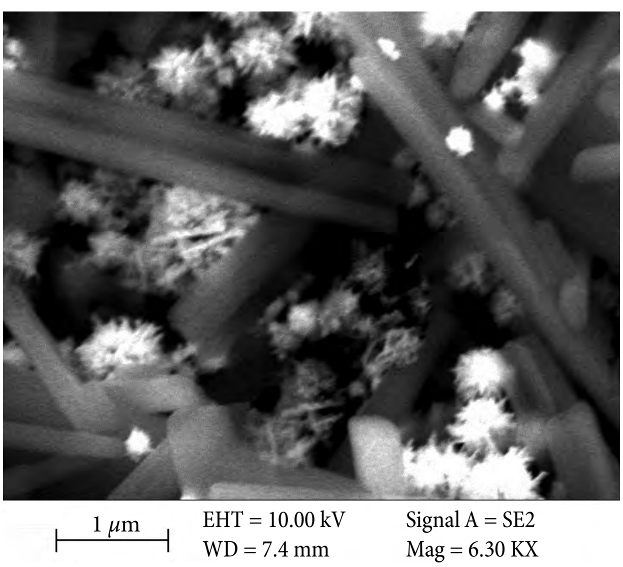

Fig. 4. The SEM image of a thin film of the C_{60}–Ag nanocomposite formed by thermal evaporation at ~45°C.

The absorption spectra of C_{60}–Ag thin films on the substrate were studied at the fixed Ag concentration (0.08 mg/ml). Figure 5 shows the absorption spectra of a thin film of fullerene C_{60} (curve *1*), a nanocomposite film C_{60}–Ag at room temperature (curve *2*), and after annealing at 60°C (curve *3*). The absorption spectrum of the pure fullerene C_{60} thin film shows two absorption lines in a range of ~346 and ~443 nm. It was found that at 0.08 mg/ml Ag concentration in the C_{60}–Ag thin film at room temperature, an increase in absorption and the appearance of a characteristic localized surface plasmon resonance (LSPR) band are observed (Fig. 5, curve *2*). In this case, the characteristic LSPR band appears at ~480 nm. The clearer appearance of the LSPR band in the film with 0.08 mg/ml Ag compared to the C_{60}/xylene/Ag/ethanol solution (see Fig. 2) indicates that the distribution of nanoparticles in the film and its structure have changed. In this case, the interaction between the C_{60} molecular orbitals and the AgNP plasmonic field leads to the plasmon–exciton coupling, effectively amplifying the optical response and increasing the oscillator strength of fullerene transitions [26].

To better understand the nature of the SPR bands in the film, it was studied after annealing at 60°C for 40 min. Thermal treatment results in a substantial increase in the overall absorption intensity, a noticeable sharpening of the absorption features, and the LSPR is clearly visible at ~492 nm (see Fig. 5, curve *3*). These changes indicate an improved structural organization of the composite film. Annealing likely induces the enhanced crystallinity of C_{60} domains, the partial coalescence of Ag nanoparticles, and the strengthening of interfacial Ag–C_{60} electronic coupling. Consequently, the annealed film exhibits the highest optical density among the three samples. Enhanced absorption in both as-deposited and annealed Ag–C_{60} films is the result of the combined effects of crystalline C_{60}NWs, plasmonic Ag nanoparticles distributed along the C_{60} matrix, and the enhancement of the Ag-induced exciton field. Thermal annealing further enhances these interactions, resulting in a more optically active and structurally superior film.

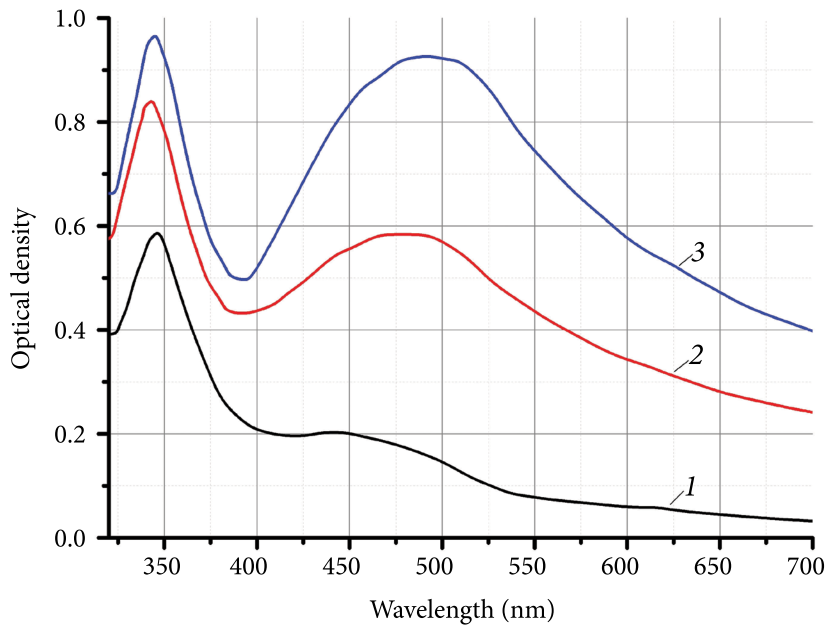

Fig. 5. UV–visible absorption spectra of a thin film of pure C_{60} fullerene (curve *1*), a C_{60}–Ag thin film at room temperature (*2*) and after annealing of a C_{60}–Ag thin film at 60°C (*3*). The concentration of C_{60} and Ag in the initial solution were 0.2 and 0.08 mg/ml, respectively.

The analysis of the Raman spectra of the C_{60} film and the C_{60}–Ag film allows us to determine the charge transfer between these particles. Figure 6 shows the Raman spectra of studied thin films. It can be seen that for the C_{60} film, there are vibrations at frequencies of ~1422 ($H_g(7)$ vibrational mode), ~1464 ($A_g(2)$) and ~1572 cm^{-1} ($H_g(8)$). The Raman spectrum of the C_{60}–Ag thin film has changed significantly due to the interaction of nanoparticles compared with that of the pure C_{60} film. The latter arises as a result of the decrease in symmetry and the weakening of the selection rule during the adsorption of fullerene C_{60} on the nanocomposite. The C_{60}–Ag composite film shows a clear downshift of the $A_g(2)$ mode to lower wavenumbers together with a pronounced broadening of the band that manifests as an apparent splitting into two components at ~1460 and ~1464 cm^{-1} (Fig. 6). Such changes in the $A_g(2)$ vibrational line are widely recognized as fingerprints of charge transfer between metals and fullerene molecules [27].

The downshift of the $A_g(2)$ band, in our opinion, arises from the electron (charge) donation from silver nanoparticles into the LUMO of C_{60}, partially filling antibonding orbitals and thereby softening the intramolecular C–C vibrations. It should be noted that the charge transfer across the interface from metal to fullerene occurs due to the difference in the Fermi energy level of silver and the LUMO of C_{60}.

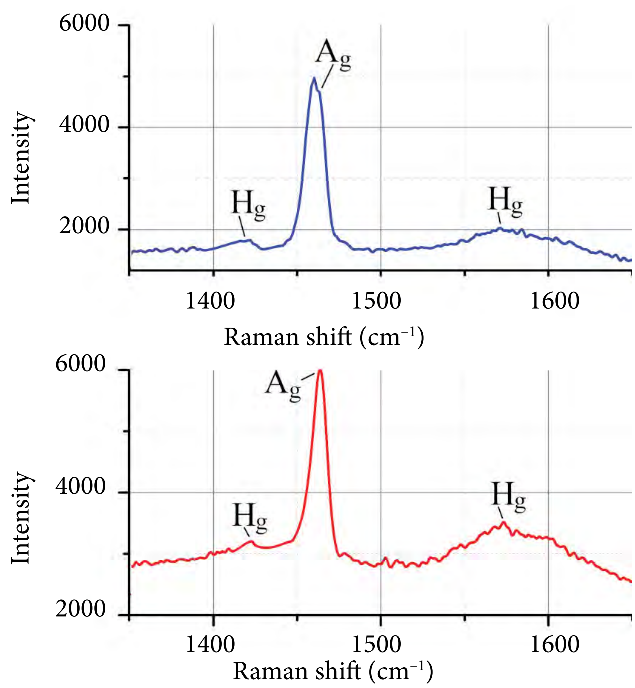

Fig. 6. Raman spectra of a thin film of C_{60} (down curve) and a C_{60}–Ag nanocomposite (top curve) containing 0.08 mg/ml Ag. The concentration of C_{60} in the solution was 0.2 mg/ml.

The stability of the structure of C_{60}–Ag nanomaterials to thermal, mechanical and ion bombardment effects require detailed studies. This is an excellent area for further research.

4. Conclusions

This work presents the results of research on the synthesis of supramolecular structures based on fullerene C_{60} and silver nanoparticles. The morphological and optical properties of C_{60}–Ag structures both in solutions and on the solid substrate surfaces were studied in detail. The interactions between fullerene and silver nanoparticles are analyzed. The obtained results emphasize the importance of interparticle interactions in controlling the process of obtaining C_{60} and metal-containing nanomaterials and open up the possibility of using the concentration of components from low to high as a parameter. This concept is valuable in obtaining nanomaterials for biomedicine, photodynamic therapy, pharmacology, electronics, sensors, and other modern applications.

Aknowledgements

This work was supported by a project of the Ministry of Higher Education, Science and Innovation Republic of Uzbekistan (Project FL-8323102108, for 2024–2028), Intergovernmental Cooperation Projects in the National Key Research and Development Plan of the Ministry of Science and Technology of PRC (Project 2022YFE0196800, for 2023–2025) and by the Foundation for Fundamental Research of the Academy of Sciences of the Republic of Uzbekistan.

References

[1] R.G. Mendes, P.S. Wróbel, A. Bachmatiuk, J. Sun, T. Gemming, Z. Liu, and M.H. Rümmeli, Carbon nanostructures as a multi-functional platform for sensing applications, Chemosensors **6**, 60 (2018), https://doi.org/10.3390/chemosensors6040060

[2] A.G. Olabi, Q. Abbas, M.A. Abdelkareem, A.H. Alami, M. Mirzaeian, and E.T. Sayed, Carbon-based materials for supercapacitors: recent progress, challenges and barriers, Batteries **9**, 19 (2023), https://doi.org/10.3390/batteries9010019

[3] S.A. Bakhramov, U.K. Makhmanov, and B.A. Aslonov, The synthesis of C_{70} fullerene nanowhiskers using the evaporating drop method, Condens. Matter **8**, 62 (2023), https://doi.org/10.3390/condmat8030062

[4] P.A. Kumar, V.V. Namboodiri, G. Joshi, and K.P. Mehta, Fabrication and applications of fullerene-based metal nanocomposites: A review, J. Mater. Res. **36**, 114 (2021), https://doi.org/10.1557/s43578-020-00094-1

[5] G. Orlandi and F. Negri, Electronic states and transitions in C_{60} and C_{70} fullerenes, Photochem. Photobiol. Sci. **1**, 289 (2002), https://doi.org/10.1039/B200178K

[6] L. Benatto, C.F.N. Marchiori, T. Talka, M. Aramini, N.A.D. Yamamoto, S. Huotari, L.S. Roman, and M. Koehler, Comparing C_{60} and C_{70} as acceptor in organic solar cells: Influence of the electronic structure and aggregation size on the photovoltaic characteristics, Thin Solid Films **697**, 137827 (2020), https://doi.org/10.1016/j.tsf.2020.137827

[7] L. Wang and Y. Liu, Electrocatalytic innovations at atomic scale: from single-atom to periodic ensembles for sustainable energy conversion, Nanomaterials **15**, 634 (2025), https://doi.org/10.3390/nano15080634

[8] R. Vishnoi, K. Sharma, S. Yadav, and R. Singhal, Investigation of sequential thermal annealing effect on Cu-C_{70} nanocomposite thin film, Thin Solid Films **680**, 75 (2019), https://doi.org/10.1016/j.tsf.2019.04.004

[9] M. Prosa, M. Bolognesi, L. Fornasari, G. Grasso, L. Lopez-Sanchez, F. Marabelli, and S. Toffanin, Nanostructured organic/hybrid materials and components in miniaturized optical and chemical sensors, Nanomaterials **10**, 480 (2020), https://doi.org/10.3390/nano10030480

[10] A. Loiseau, V. Asila, G. Boitel-Aullen, M. Lam, M. Salmain, and S. Boujday, Silver-based plasmonic nanoparticles for and their use in biosensing, Biosensors **9**, 78 (2019), https://doi.org/10.3390/bios9020078

[11] H. Yi, R. Liu, Z. Chen, and B. Nie, Visible-light driven photodegradation on Ag nanoparticle-embedded fullerene (C_{60}) heterostructural

microcubes, Chemosphere **258**, 127355 (2020), https://doi.org/10.1016/j.chemosphere.2020.127355

[12] X.Q. Shi, M.A. Van Hove, and R.Q. Zhang, Survey of structural and electronic properties of C_{60} on close-packed metal surfaces, J. Mater. Sci. **47**, 7341 (2012), https://doi.org/10.1007/s10853-012-6361-y

[13] A. Mahor, P.P. Singh, P. Bharadwaj, N. Sharma, S. Yadav, J.M. Rosenholm, and K.K. Bansal, Carbon-based nanomaterials for delivery of biologicals and therapeutics: A cutting-edge technology, C-J. Carbon Res. **7**, 19 (2021), https://doi.org/10.3390/c7010019

[14] S.P. Vinay, Synthesis of fullerene (C_{60})-silver nanoparticles using neem gum extract under microwave irradiation, J. BioNanoSci. **11**, 1 (2021), https://doi.org/10.1007/S12668-020-00799-X

[15] K.L. Kelly, E. Coronado, L.L. Zhao, and G.C. Schatz, The optical properties of metal nanoparticles: The influence of size, shape, and dielectric environment, J. Phys. Chem. B **107**, 668–677 (2003), https://doi.org/10.1021/jp026731y

[16] D.D. Evanoff and G. Chumanov, Synthesis and optical properties of silver nanoparticles and arrays, ChemPhysChem **6**, 1221–1231 (2005), https://doi.org/10.1002/cphc.200500113

[17] P.K. Jain, K.S. Lee, I.H. El-Sayed, and M.A.J. El-Sayed, Calculated absorption and scattering properties of gold nanoparticles of different size, shape, and composition: Applications in biological imaging and biomedicine, Phys. Chem. B **110**, 7238–7248 (2006), https://doi.org/10.1021/jp057170o

[18] V. Amendola and M. Meneghetti, Laser ablation synthesis in solution and size manipulation of noble metal nanoparticles, Phys. Chem. Chem. Phys. **11**, 3805–3821 (2009), https://doi.org/10.1039/b900654k

[19] S. Link and M.A. El-Sayed, Optical properties and ultrafast dynamics of metallic nanocrystals, Annu. Rev. Phys. Chem. **54**, 331–366 (2003), https://doi.org/10.1146/annurev.physchem.54.011002.103759

[20] D. Paramelle, A. Sadovoy, S. Gorelik, P. Free, J. Hobley, and D.G. Fernig, A rapid method to estimate the concentration of citrate capped silver nanoparticles from UV-visible light spectra, Analyst **139**, 4855–4861 (2014), https://doi.org/10.1039/C4AN00978A

[21] U.K. Makhmanov, A.M. Kokhkharov, S.A. Bakhramov, S.A. Esanov, and D. Erts, Self-assembly of C_{60} fullerene molecules in the hexane–xylene solvent system, Fullerenes, Nanotubes, Carbon Nanostruct. **30**, 80 (2022), https://doi.org/10.1080/1536383X.2021.1992390

[22] V. Lavrentiev, D. Chvostova, J. Pokorny, I. Lavrentieva, J. Vacik, and A. Dejneka, Tuneable interplay of plasmonic and molecular excitations in self-assembled silver-fullerene nanocomposites, Carbon **184**, 34 (2021), https://doi.org/10.1016/j.carbon.2021.08.002

[23] Y. Wang, Z. Gao, Z. Han, Y. Liu, H. Yang, T. Akkin, C.J. Hogan, and J.C. Bischof, Aggregation affects optical properties and photothermal heating of gold nanospheres, Sci. Rep. **11**, 898 (2021), https://doi.org/10.1038/s41598-020-79393-w

[24] P. Merkl, S. Zhou, A. Zaganiaris, M. Shahata, A. Eleftheraki, T. Thersleff, and G.A. Sotiriou, Plasmonic coupling in silver nanoparticle aggregates and their polymer composite films for near-infrared photothermal biofilm eradication, ACS Appl. Nano Mater. **4**, 5330 (2021), https://doi.org/10.1021/acsanm.1c00668

[25] A. Capocefalo, T. Bizien, S. Sennato, N. Ghofraniha, F. Bordi, and F. Brasili, Responsivity of fractal nanoparticle assemblies to multiple stimuli: structural insights on the modulation of the optical properties, Nanomaterials (Basel) **12**, 1529 (2022), https://doi.org/10.3390/nano12091529

[26] V. Lavrentiev, J. Pokorny, D. Chvostova, M. Klementova, I. Lavrentieva, J. Vacik, and A. Dejneka, Relevance of Rabi splitting effect for tunable enhancement of Raman scattering in self-assembled silver – fullerene nanocomposite films, Carbon **196**, 988 (2022), https://doi.org/10.1016/j.carbon.2022.06.002

[27] R.P. Pandeya, K.P. Shchukin, Y. Falke, G. Mussler, A.R. Jalil, N. Atodiresei, E.H. Hasdeo, A. Fedorov, B.V. Senkovskiy, D. Jansen, G.D. Santo, and L. Petaccia, Molecular order induced charge transfer in a C_{60}-topological insulator Moiré heterostructure, Nano Lett. **25**, 1220 (2025), https://doi.org/10.1021/acs.nanolett.4c06294

ANGLIES NANODARINIŲ SU SIDABRU PARUOŠIMAS IR CHARAKTERIZAVIMAS

U.K. Makhmanov [a, b], Xiaohong Jiang [c], Jiazhi Yang [c], T.A. Chuliev [a]

[a] *Uzbekistano mokslų akademija, Taškentas, Uzbekistanas*

[b] *Nacionalinis Mirzo Ulugbeko universitetas, Taškentas, Uzbekistanas*

[c] *Nandzingo mokslo ir technologijos universitetas, Nandzingas, Kinija*